Thermal analysis of the TOF lead target at CERN

C. Aragonese, S. Buono, L. Maciocco, V. Moreau, L. Sorrentino
CRS4, Centre for Advanced Studies, Research and Development in Sardinia

G. Garcia-Munoz, V. Lacoste
CERN, European Organization for Nuclear Research

Cagliari, 16th March 2001

Abstract

The lead target at the Time Of Flight (TOF) facility at CERN, currently under commissioning, undergoes relevant temperature transients due to the intensity of the four 20 GeV/c pulses of 7 x 10^{12} protons, carrying an energy of 21.4 kJ delivered in 7 ns each.

A 3D thermal analysis of the target system in both steady-state and transient conditions has been performed using the finite volume commercial code StarCD coupled with the results from Fluka simulations.

Results show that the maximum temperature inside the lead target using the parameters of the TOF commissioning phase (4 pulses every 1.2 s in a 14.4 s super-cycle) is 127 ^{o}C at steady-state operations, which is an acceptable value, compatible with safe and durable target operations. A significant improvement could be obtained by doubling the beam size (108 ^{o}C maximum temperature in the bulk of the central block).

The transients coming from the pulsed operation are not such as to create structural problems related to thermal fatigue. It is interesting to notice that the thermal oscillation in the hottest point in the bulk of the central block is much lower in the case where the 4 pulses are spaced of 3.6 s during the PS super-cycle (about 20 ^{o}C), than in the case where they are spaced of only 1.2 s (about 40 ^{o}C).

1 Introduction

The TOF [1] lead target, currently under commissioning at CERN, undergoes relevant temperature transients due to the intensity of the 20 GeV/c incident beam. In fact a pulse of 7 x 10^{12} protons carries an energy of 21.4 kJ delivered in 7 ns. In the actual beam size and distribution, this causes a maximum theoretical (adiabatic) temperature increase of 20 ^{o}C inducing a relevant dynamic transient.

Therefore, it is important to evaluate the operating temperatures of the target not only in steady-state conditions, but also during transients. Our scope is to assess the average operating temperature and the thermal fatigue of the system in different target operating conditions.

These calculations are also necessary to give input for study of the propagation of elastic waves and the corresponding stresses induced in order to assess the eventuality of a mechanical failure [2].

2 The spallation target

The spallation target is a pure lead block of cubic shape of dimensions 80x80x60 cm^3 (see figures 1 to 4). The proton beam hits the target surface in the front face, where a volume of dimensions 30x55x20 cm^3 was removed in the spallation zone. The beam direction makes an angle of 10 degrees with respect to the normal to the surface.

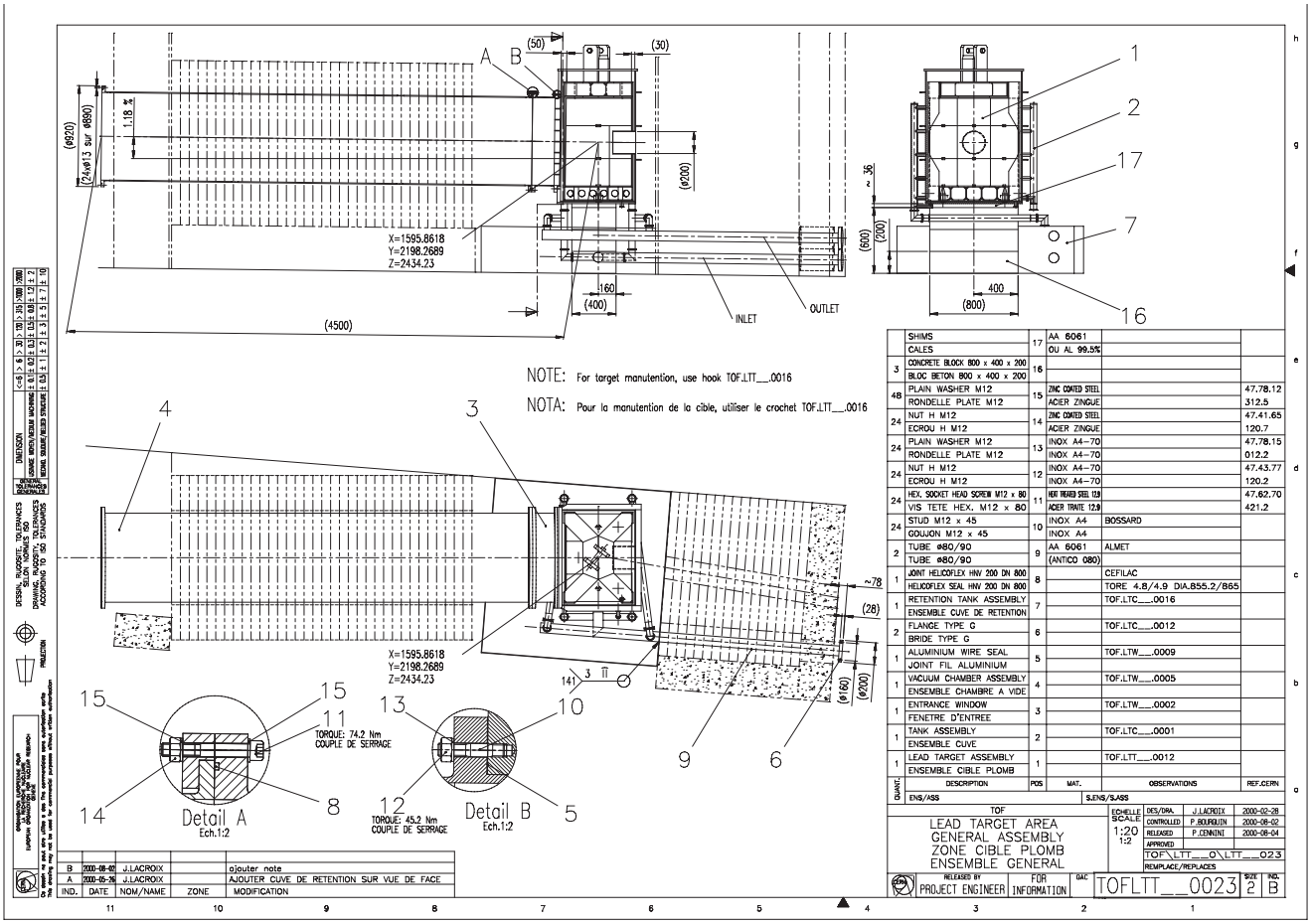

Figure 1: General Assembly.

The power dissipation of the incident beam in the target gives rise to a sensible temperature increase and therefore requires cooling. In extreme conditions up to 4 bunches per supercycle at 20 GeV/c could be delivered spaced with a minimum of 1.2 s with a total yield of 2.8×10^{13} protons. The average beam current will be about 0.31 μA, and the beam energy in a supercycle will reach about 85.6 kJ. According to simulations with the FLUKA Monte-Carlo code [4], the power deposit in the target is about 51% of the beam power, some 3.03 kW in such conditions.
The cooling of the lead target will be made by circulating a 3 cm thick layer of demineralized water (6 l/s flow rate) around the target except for the TOF face, where the water layer will be 5 cm for neutron moderation. The lead target is immersed in an aluminium tank whose walls are 0.5 cm thick.

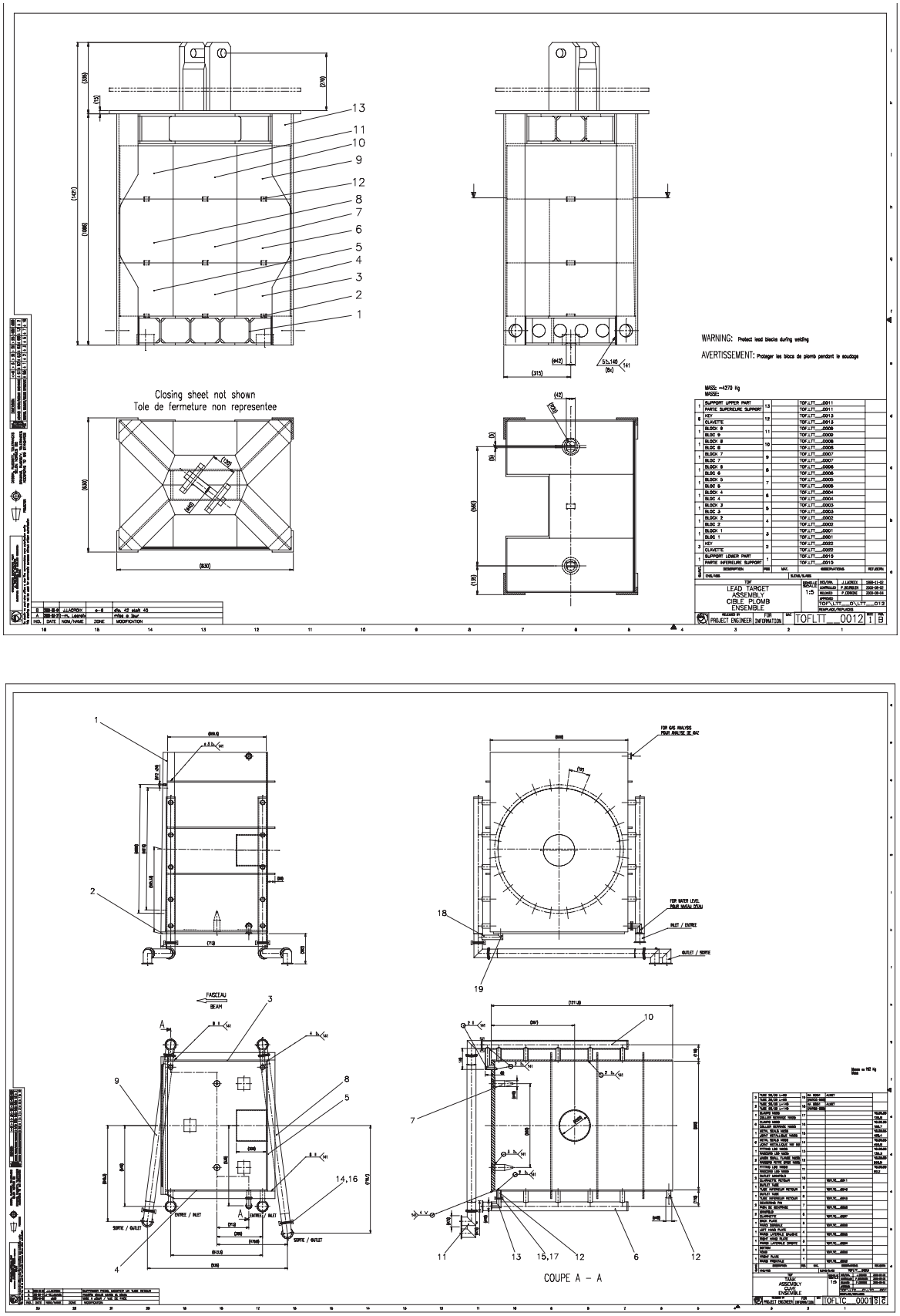

Figure 2: Target and window assemblies.

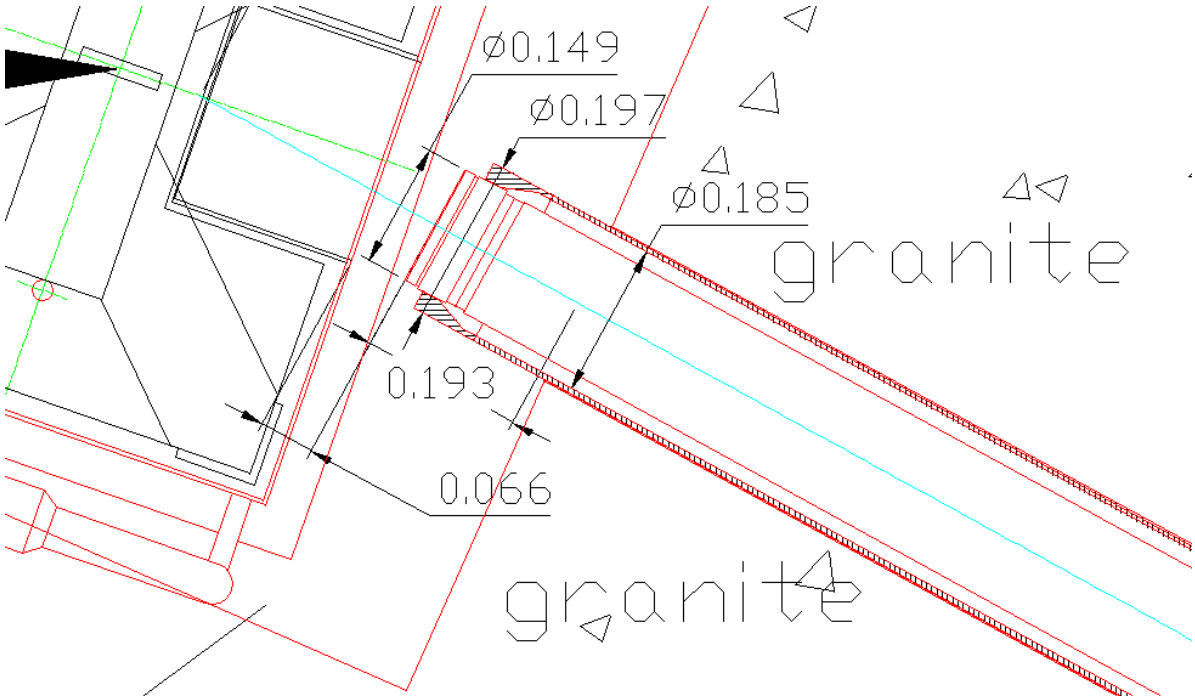

Figure 3: Detail of the beam transport tube.

3 FLUKA simulation

3.1 The proton beam

The simulation for the energy deposition in the lead target was first performed using the beam characteristics given by the CERN PS (Table 1). The momentum of the protons is of 20 GeV/c, with a FWHM of 0.1413. The nominal size of the beam at the target is such as FWHM (v) = 1.3188 cm and FWHM (h) = 1.8369 cm. The origin of the system is in the centre of the lead target; the proton beam travels in the Z direction with an incident angle of 10°, the X-axis is vertical and the Y-axis points to the right. The beam hits the lead target at the point (x = 0, y = -1.7632 cm, z = -10 cm).

Transverse parameters		Longitudinal parameters	Beam size at target	
σ_H (1σ)[mm mrad]	1.88	dp/p $\pm 3\times10^{-3}$	σ_H [mm]	7.8
σ_V(1σ) [mm mrad]	1.41		σ_V [mm]	5.6

Table 1: Beam parameters used for the computation of the beam envelope, together with the beam size at the target location.

To estimate the impact on maximum operating temperatures, further simulations were performed with different proton beam dimensions given in Table 2.

	$\sigma_{commissioning}$	$\sigma_c/2$	$\sigma_c\times2$
σ_H [mm]	12.2	6.1	24.4
σ_V [mm]	6	3	12

Table 2: Proton beam size used in FLUKA simulations for a parametrical study of the lead target temperature behaviour.

3.2 Geometry of the target

The geometry used in the FLUKA simulation is showed in figure 4. The lead target is immersed in an aluminium tank where a demineralized water flow is provided. The water layer surrounding the lead block is 3 cm thick except at the exit face of the target where it is 5 cm thick. The walls of the aluminium container are 0.5 cm thick.

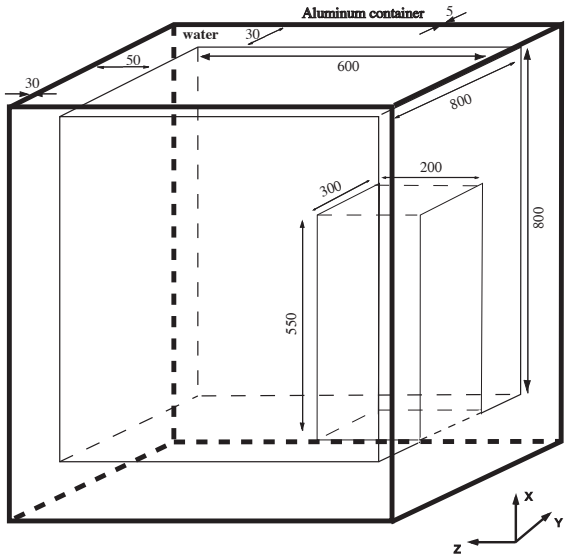

Figure 4. Geometry of the simulated lead target.

3.3 Binning structure and energy deposition

The lead target has been divided into 17 regions; three kinds of binning were used according to the desired accuracy for the energy deposition in each of them, as shown in figure 5 and in table 3. The regions were defined for z between 30 cm and -10 cm.

Block number	Block size [cm^3]	Cells number	Cell size [mm^3]
1,2,3,6,7,8,9	10x10x40	50000	4x4x4
4,5	10x10x40	$4x10^6$	1x1x1
10,12,15,17	25x25x40	100000	5x5x10
11,16	25x30x40	100000	5x6x10
13,14	30x25x40	100000	6x5x10

Table 3: regions and FLUKA cells dimensions (see also figure 5)

A last region was also defined for the proton entrance face of the target, including the window of the beam pipe, the aluminium container wall and the 3 cm of cooling water. This region, containing 96000 cells of dimension 4 mm, was not used for the calculations shown in this document.

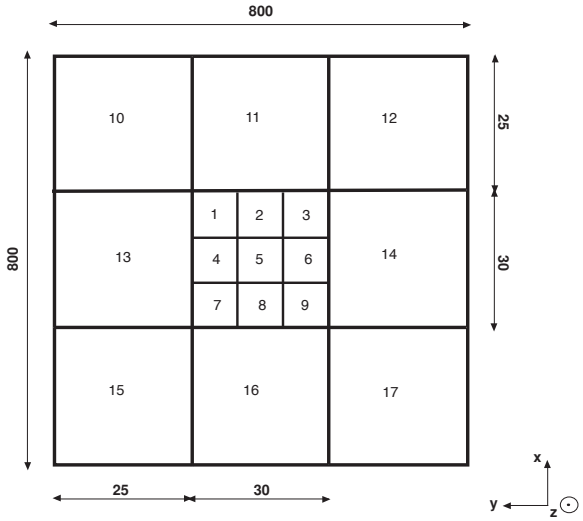

Figure 5: The lead target divided into regions with different binnings.

In the nominal conditions ($I_p = 7\times10^{12}$ p/pulse, $\sigma_H = 7.8$ mm, $\sigma_V = 5.6$ mm), the maximum energy deposit is about 4.5×10^{-2} GeV/cm^3/proton corresponding to a theoretical temperature increase of 34.4 K.
The maximum energy deposit in the lead target with the proton beam size used during the commissioning is about 2.65×10^{-2} GeV/cm^3/proton (Figure 6). This energy corresponds to a maximum temperature increase of 20.3 ^{o}C, at the nominal intensity of 7×10^{12} protons delivered per pulse.

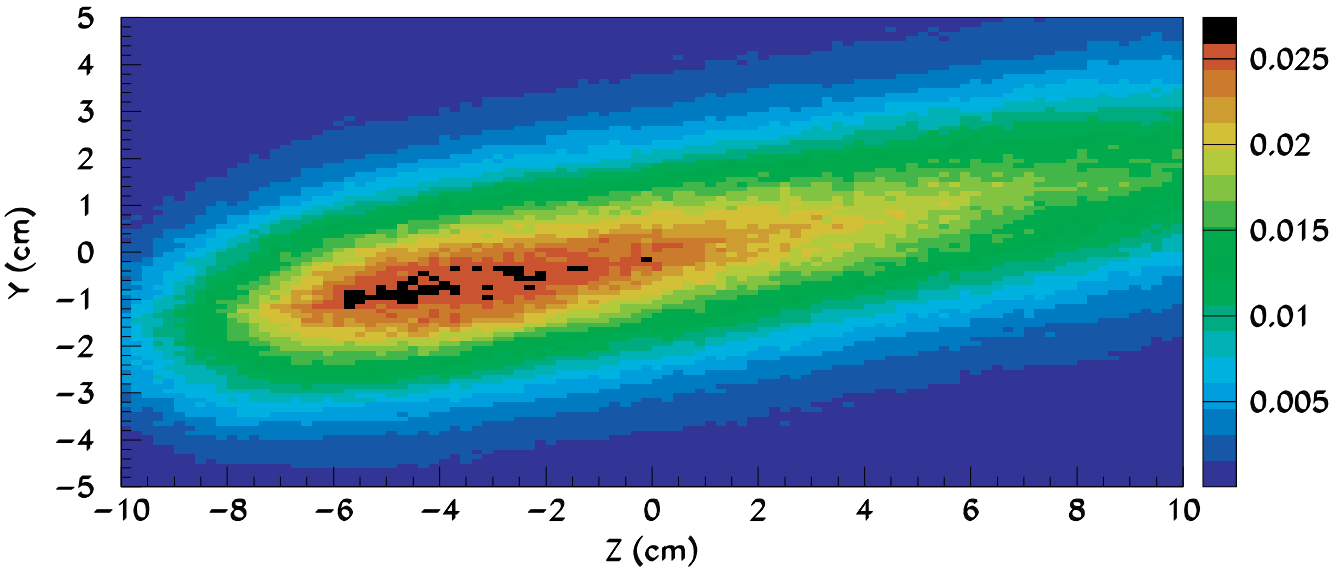

Figure 6: Maximum energy deposit in the lead target (GeV/cm^3/p 20 GeV/c) from FLUKA simulation using the proton beam size during commissioning.

4 Model set-up

A 3D thermal analysis of the target system in both steady-state and transient conditions has been performed using the finite volume commercial code StarCD [5] coupled with the results from Fluka simulations.

4.1 Lead properties

- Density: 11300 Kg/m^3
- Thermal conductivity: 27 W/m K
- Specific heat: 130 J/Kg K

4.2 Computational model and mesh

The simulations take into account only the solid lead target. The cooling water flow is simulated by imposing a temperature of 20 ^{o}C on all target walls. The energy brought into the target by the neutron beam is introduced as a source term in the lead energy equation.

A structured mesh has been used (see figure 7). The total number of elements is 73080. The cells dimensions are 1x1x1 cm^3 in the central region and about 2x2x2 cm^3 in the rest of the model. Steady-state and transient calculations were performed using the SIMPLE and PISO algorithms respectively. No convergence problems were reported.

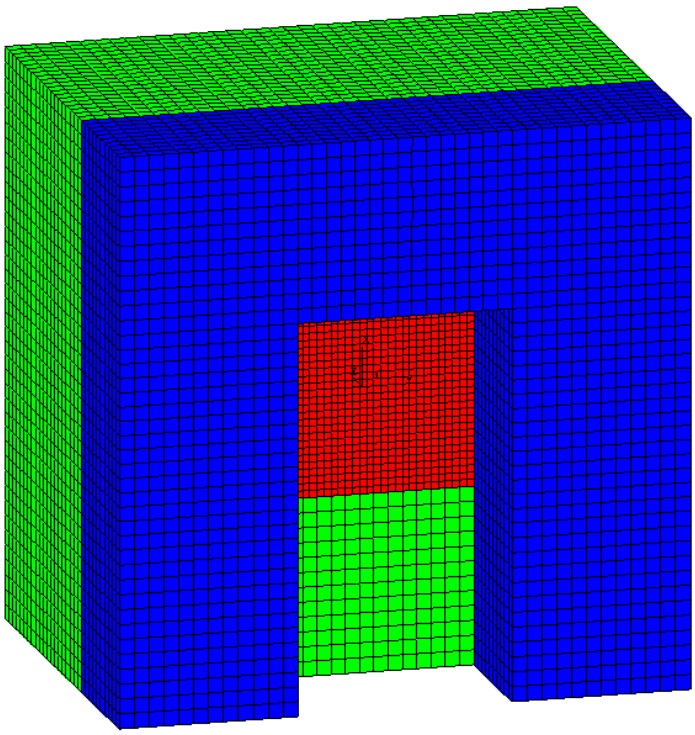

Figure 7: Computational mesh.

A series of thermo-couples were inserted into the TOF facility, as shown in figure 8. Results will be shown for these locations.

4.3 List of test-cases

Two general cases have been considered, both for steady-state and transient analysis:

- one bunch of protons every super-cycle of 14.4s;
- four bunches of protons spaced with 1.2s or 3.6s every super-cycle of 14.4 s.

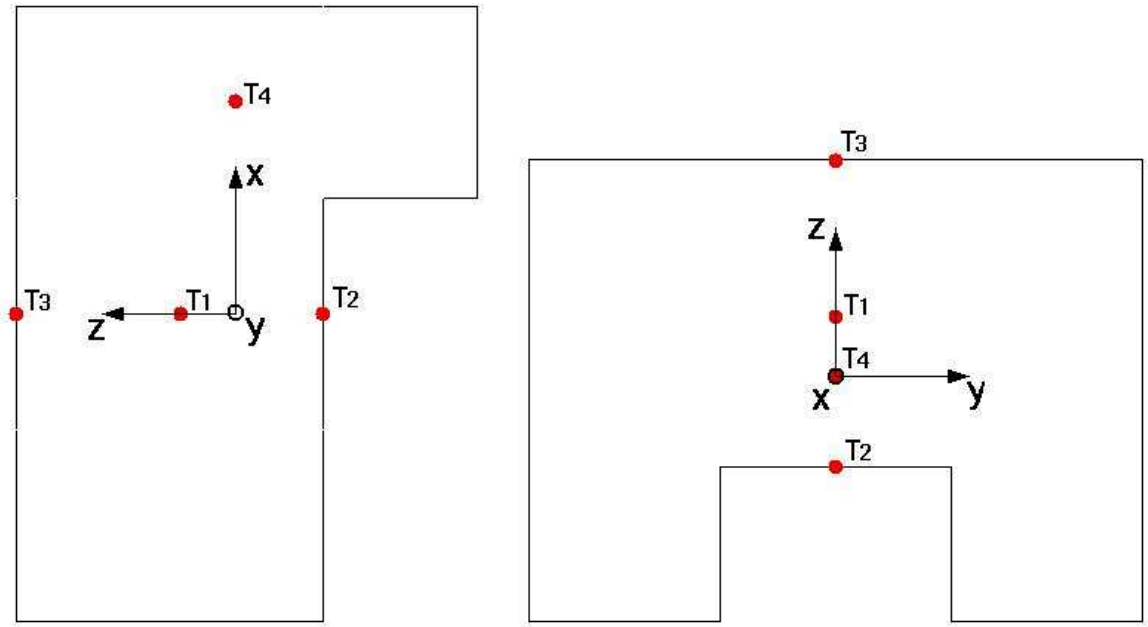

Figure 8: Reference coordinate system and thermocouples location.

All the cases considered for the present analysis are listed in table 3. In cases a-1 and b-1 a beam with half width has been considered ($\sigma_c/2$). In cases a-2 and b-2 a beam with double width has been considered ($\sigma_c \times 2$).

Case	Analysis type	Description
a	steady-state	1 bunch every super-cycle
a-1	steady-state	1 bunch every super-cycle, beam with $\sigma_c/2$
a-2	steady-state	1 bunch every super-cycle, beam with $\sigma_c \times 2$
b	steady-state	4 bunches spaced with 1.2s every super-cycle
b-1	steady-state	4 bunches spaced with 1.2s every super-cycle, beam with $\sigma_c/2$
b-2	steady-state	4 bunches spaced with 1.2s every super-cycle, beam with $\sigma_c \times 2$
c-1	transient	4 bunches spaced with 1.2s in the first super-cycle
c-2	transient	4 bunches spaced with 1.2s in one super-cycle in permanent regime
d-1	transient	4 bunches spaced with 3.6s in the first super-cycle
d-2	transient	4 bunches spaced with 3.6s in one super-cycle in permanent regime
e	transient	1 bunch every super-cycle per 100 super-cycles
f	transient	4 bunches spaced with 1.2s every super-cycle per 100 super-cycles
g	transient	30 min cooling transient starting from case a steady-state solution
h	transient	30 min cooling transient starting from case b steady-state solution

Table 4: List of calculation test cases.

5 Results

Table 4 reports the results related to the steady-state calculations. One can observe that a significant reduction in the maximum temperature can be obtained for the case where the beam size is doubled

compared to the one used in the commissioning. Nevertheless the temperature obtained in the nominal case, 124 °C, is an acceptable operating value, compatible with safe and durable target operation.

Case	Total power released [W]	Maximum temperature [C]
a	779.63	46.17
a-1	787.66	49.05
a-2	769.98	42.03
b	3118.52	124.7
b-1	3150.64	136.2
b-2	3079.93	108.1

Table 5: maximum temperatures in steady–state analysis.

The temperature distribution inside the target for case b is shown in figure 9. One can observe that the maximum temperature occurs inside the central block, while thermal gradients inside the other blocks are irrelevant. The situation is very similar in all other steady-state calculations.

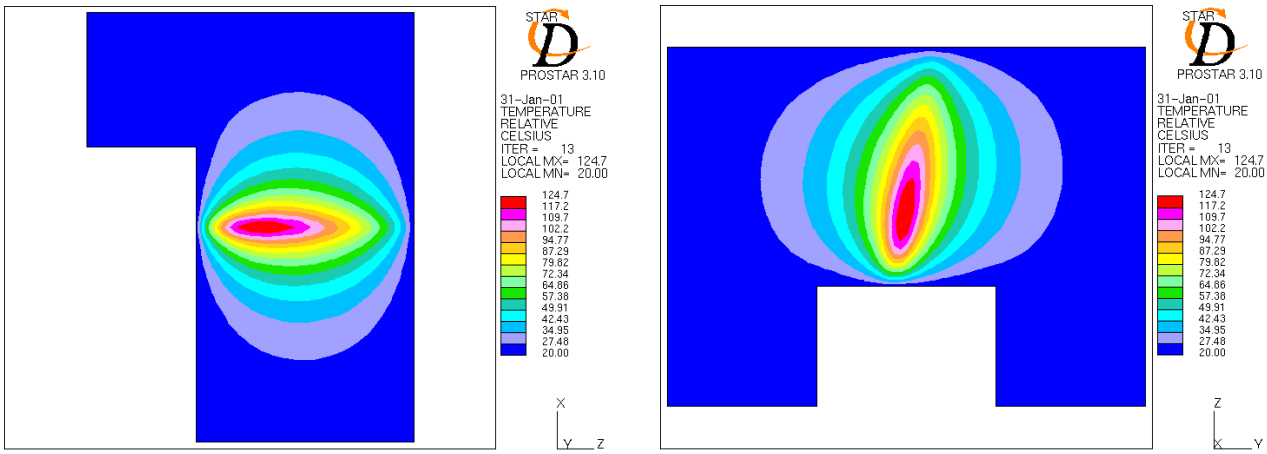

Figure 9: Case b – steady temperature distribution (horizontal and vertical view) in the target.

Figure 10 shows the temperature in relevant locations inside the target during the first super-cycle. One can observe that the temperature in the geometrical centre of the central block (thermocouple T1) is quite lower compared to the maximum temperature in the target. This is due to the 10° inclination of the beam line compared to the neutron pipe. The temperatures in the other thermocouples do not show significant variations, except for T2, which is located in the front face of the central block, closer to the interaction zone.

Figure 11 shows the same, but at steady-state operations, i.e. when the power released by the beam is equivalent to the power extracted by the water cooling system. This gives an idea of the thermal fatigue during the pulsed target operation at the maximum operating temperature. Given the fact that such temperature variation occurs inside the bulk of the central block, and that the temperature oscillation is relatively low (about 40 °C), we don't think that structural problems related to thermal fatigue can arise in these conditions.

Figures 12 and 13 show the same than figures 10 and 11 in the case where the 4 pulses occur at 3.6 s of distance during a PS super-cycle. It is interesting to notice that in this case the thermal oscillation in the hottest point in the bulk of the central block is much smaller (about 20 °C).

Figures 14 to 17 show the temperature in relevant locations inside the target during 100 super-cycles in the cases where 1 or 4 bunches per super-cycle are sent into the target. It is important to observe that,

given the large thermal capacity of the target, in the 24 minutes of continuous operation, it is still not possible to reach the steady-state temperatures. This will be possible only through much longer irradiation periods.

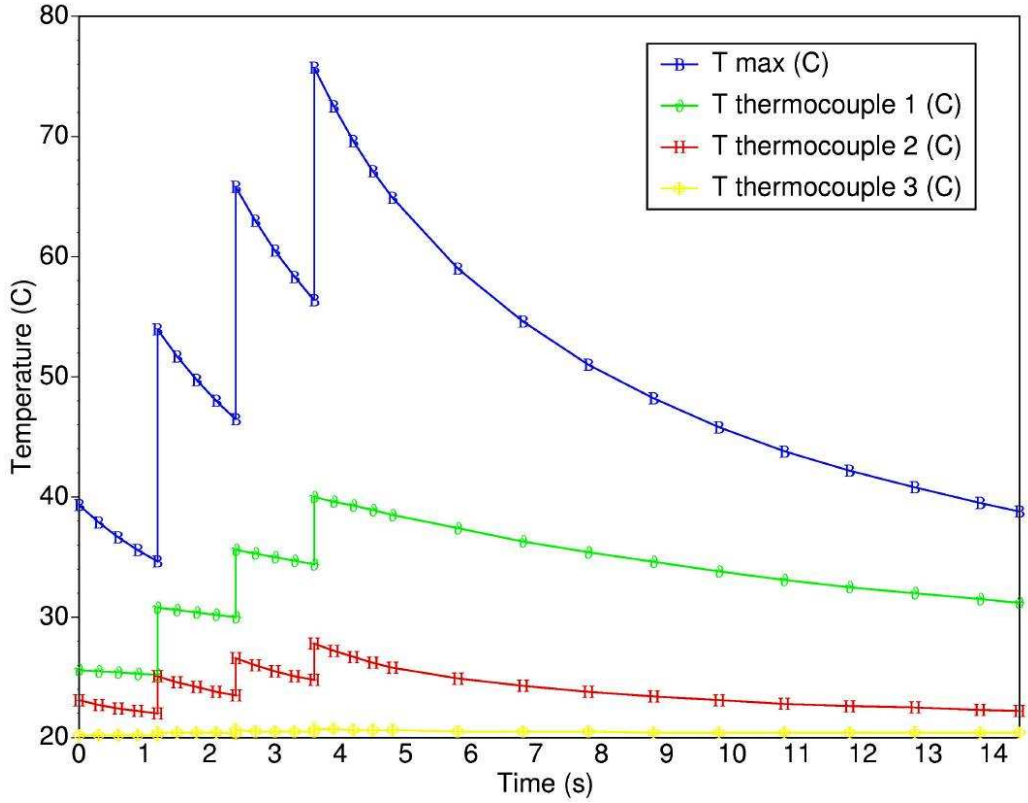

Figure 10: Case c-1 - Temperature in relevant locations inside the target during the first super-cycle. See figure 8 for thermocouples location.

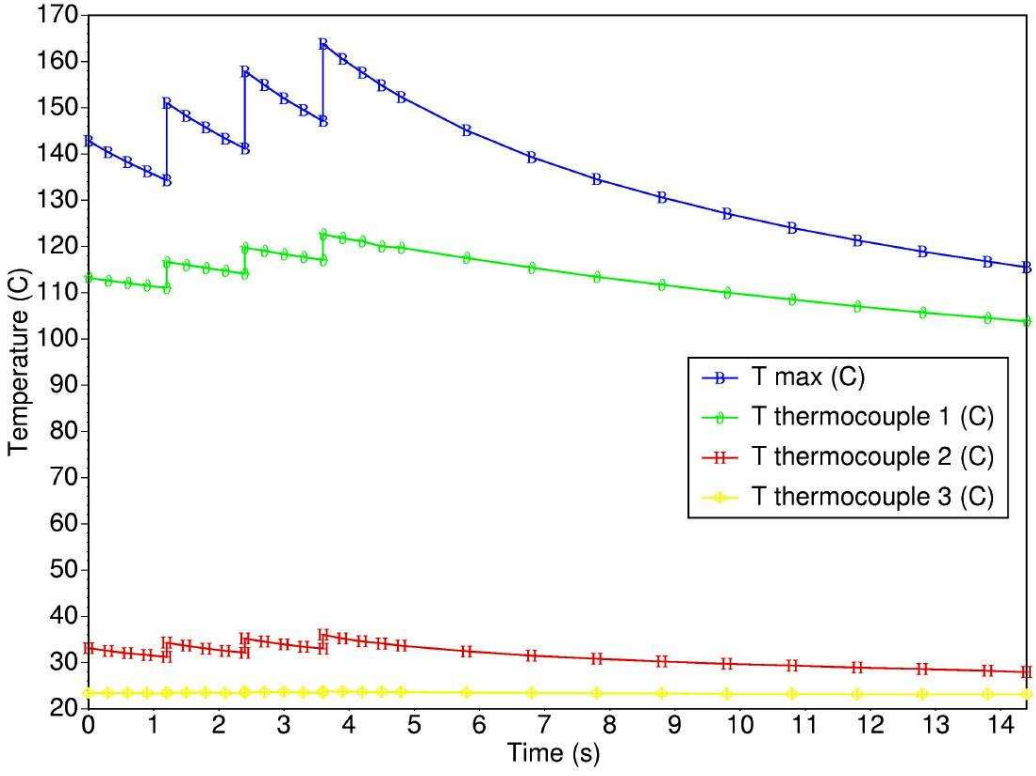

Figure 11: Case c-2 - Temperature in relevant locations inside the target during one super-cycle at steady-state operations. See figure 8 for thermocouples location.

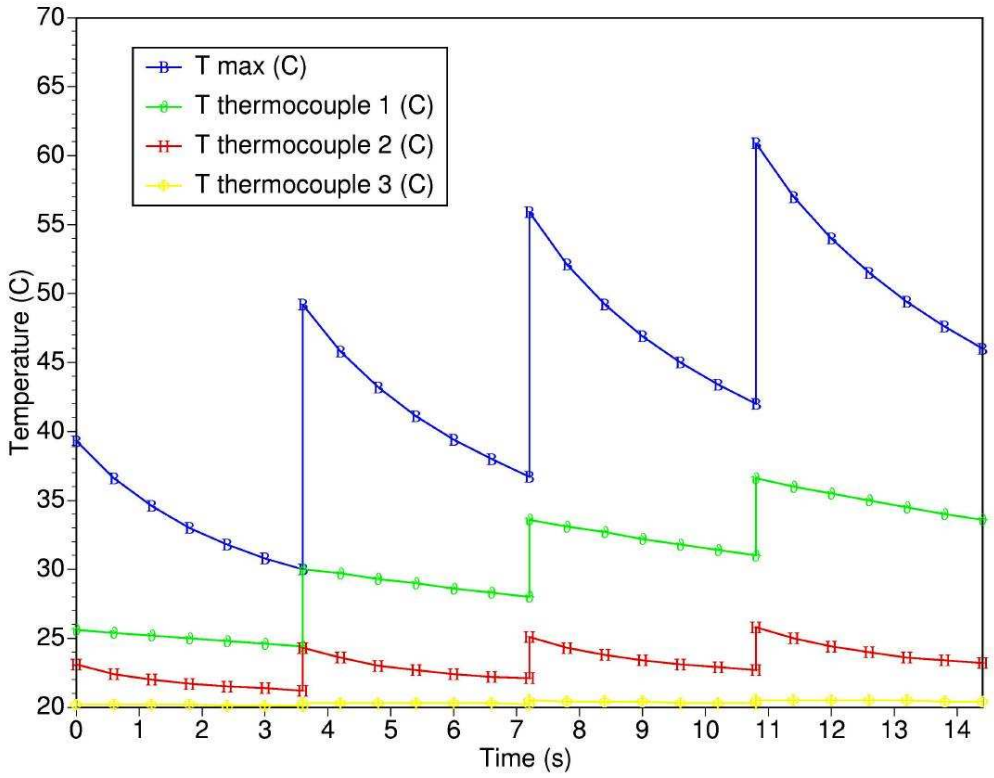

Figure 12: Case d-1 - Temperature in relevant locations inside the target during the first super-cycle (one bunch every 3.6 seconds). See figure 8 for thermocouples location.

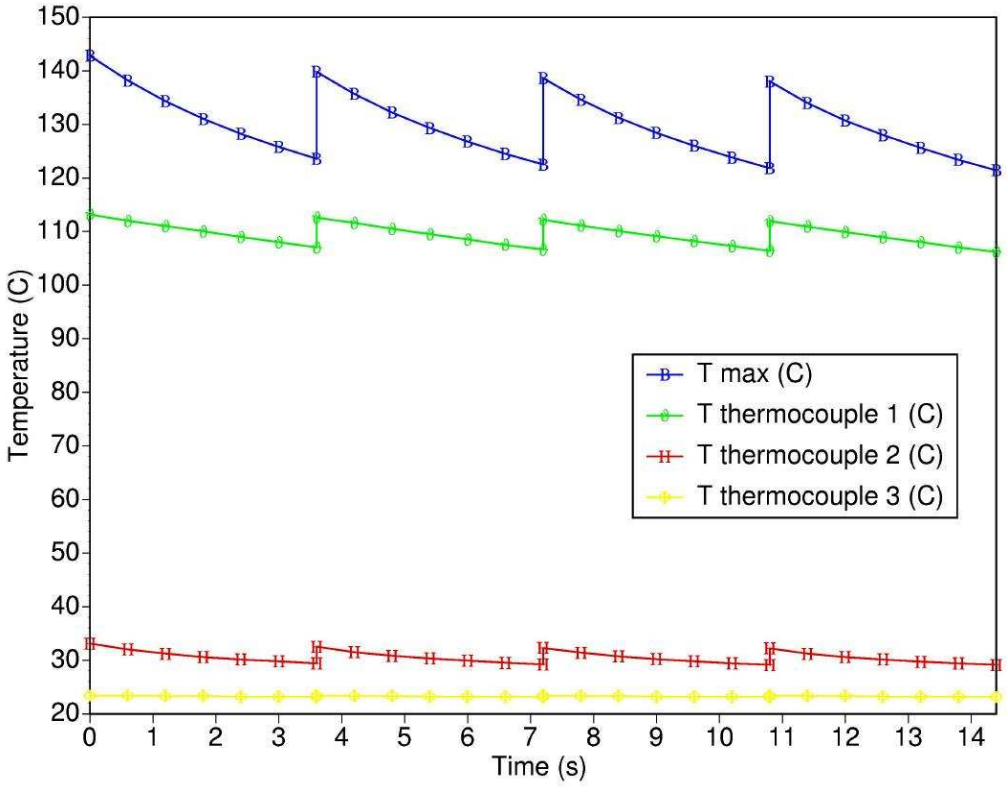

Figure 13: Case d-2 - Temperature in relevant locations inside the target during one super-cycle at steady-state conditions (one bunch every 3.6 seconds). See figure 8 for thermocouples location.

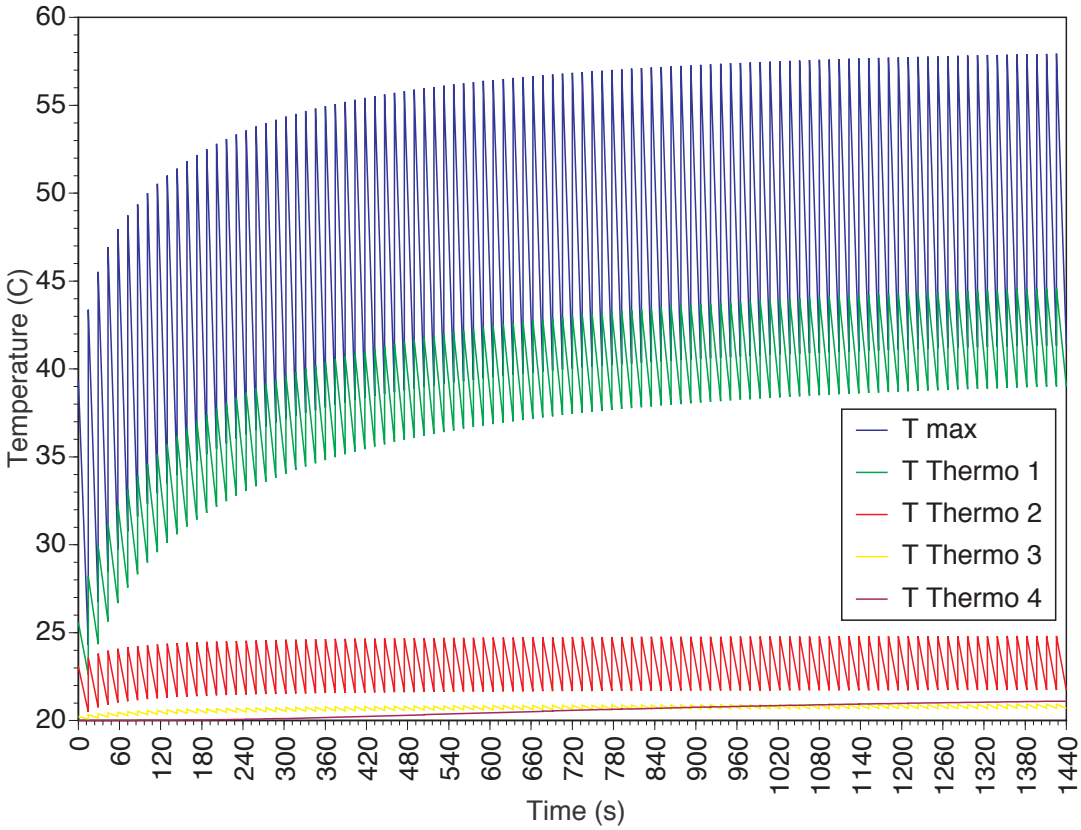
Temperature (C)
Time (s)
T max
T Thermo 1
T Thermo 2
T Thermo 3
T Thermo 4

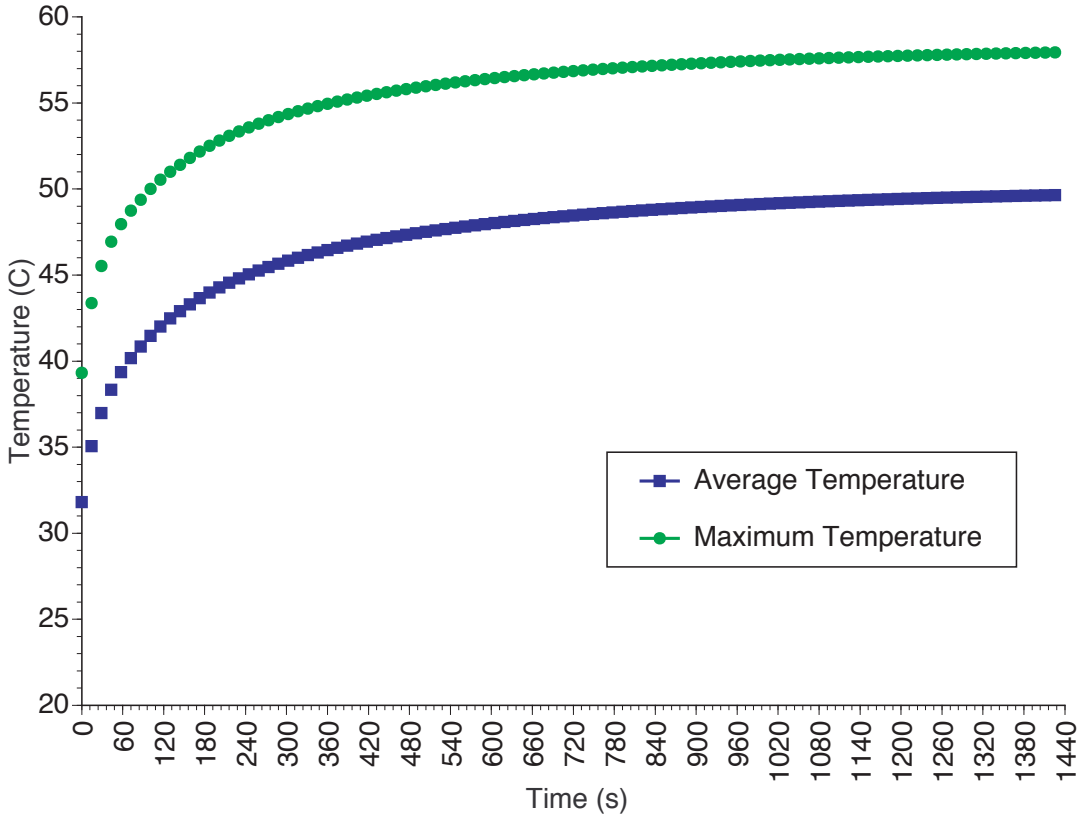
Temperature (C)
Time (s)
Average Temperature
Maximum Temperature

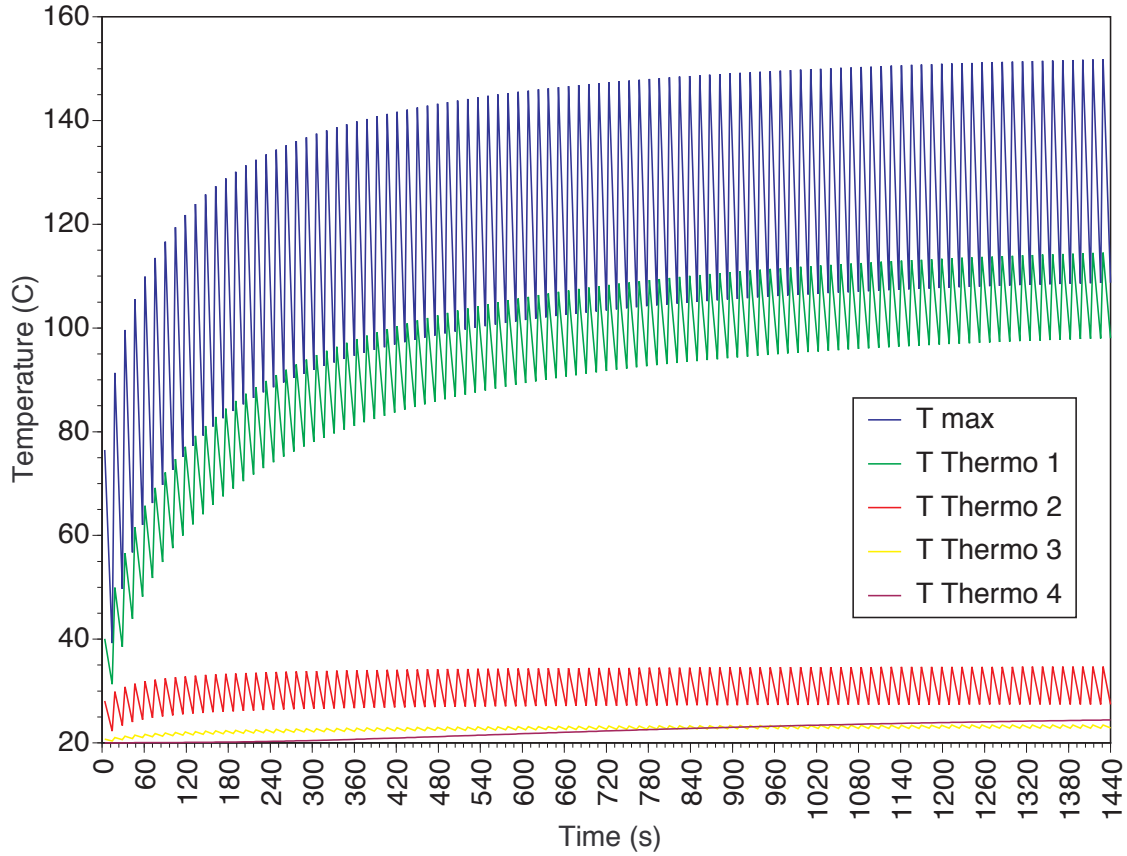
Temperature (C)
Time (s)
T max
T Thermo 1
T Thermo 2
T Thermo 3
T Thermo 4

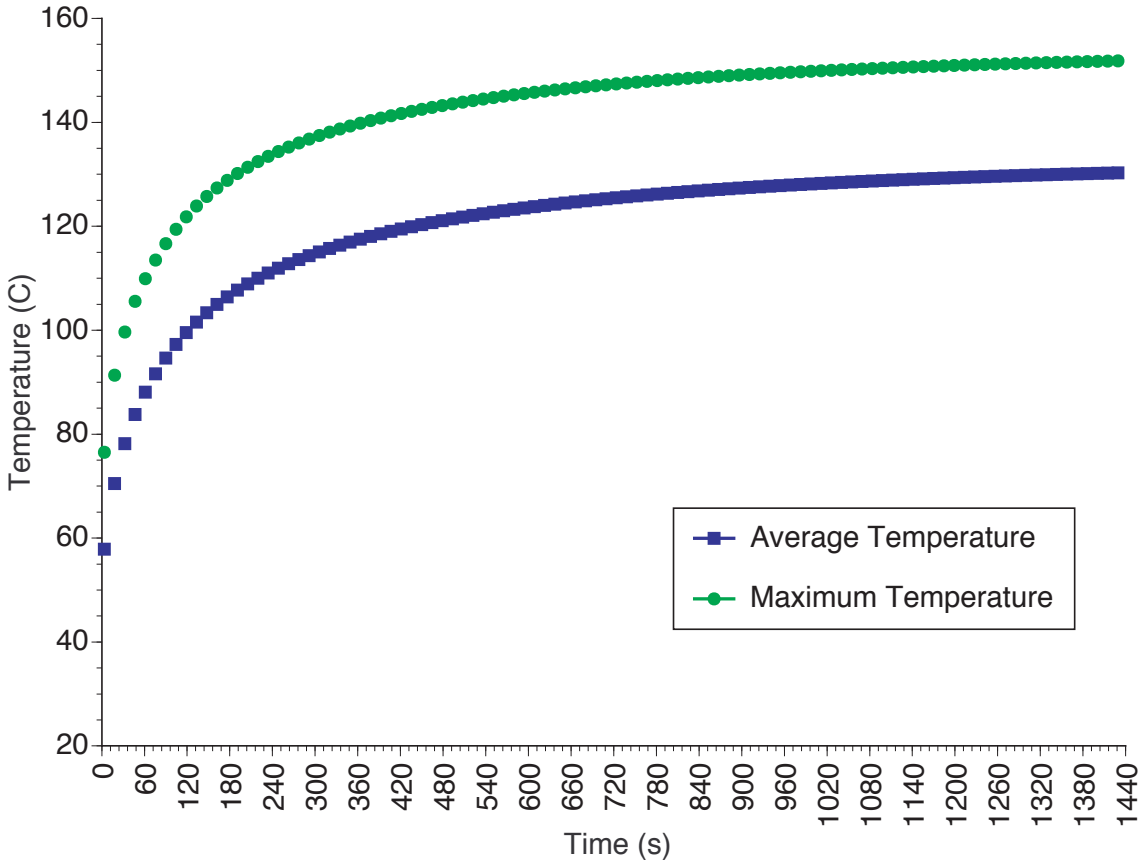
Temperature (C)
Time (s)
Average Temperature
Maximum Temperature

Figures 18 and 19 show the temperature in relevant locations inside the target during a 30 minutes cooling transient without the source term, starting from steady-state solutions in the cases where 1 or 4 bunches per super-cycle are sent into the target. It can be observed that, in this period, the temperatures lower to the initial conditions.

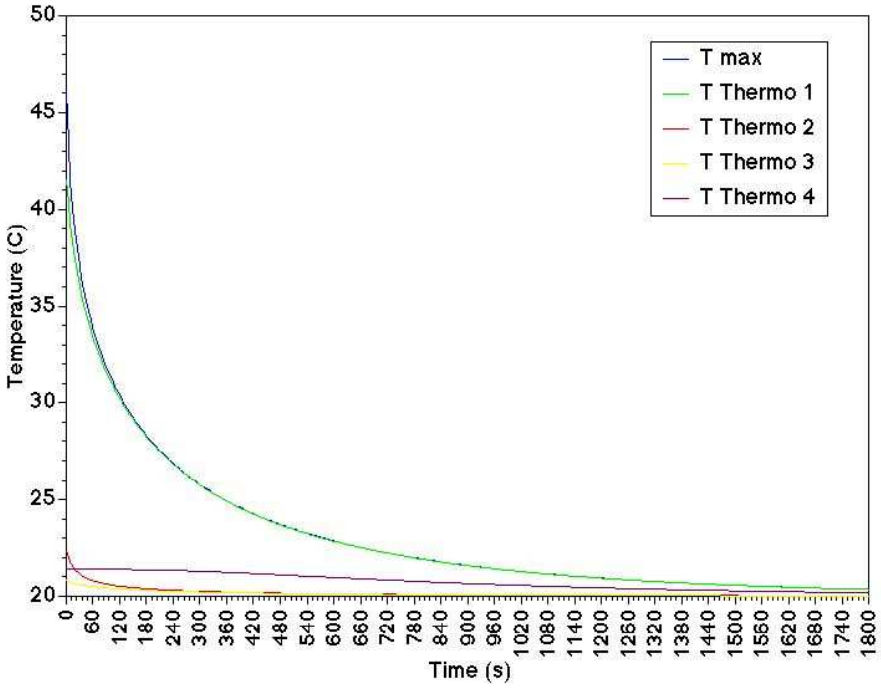

Figure 18: Case g - Temperature in relevant locations inside the target during a 30 minutes transient without the source term starting from case a steady-state solution.

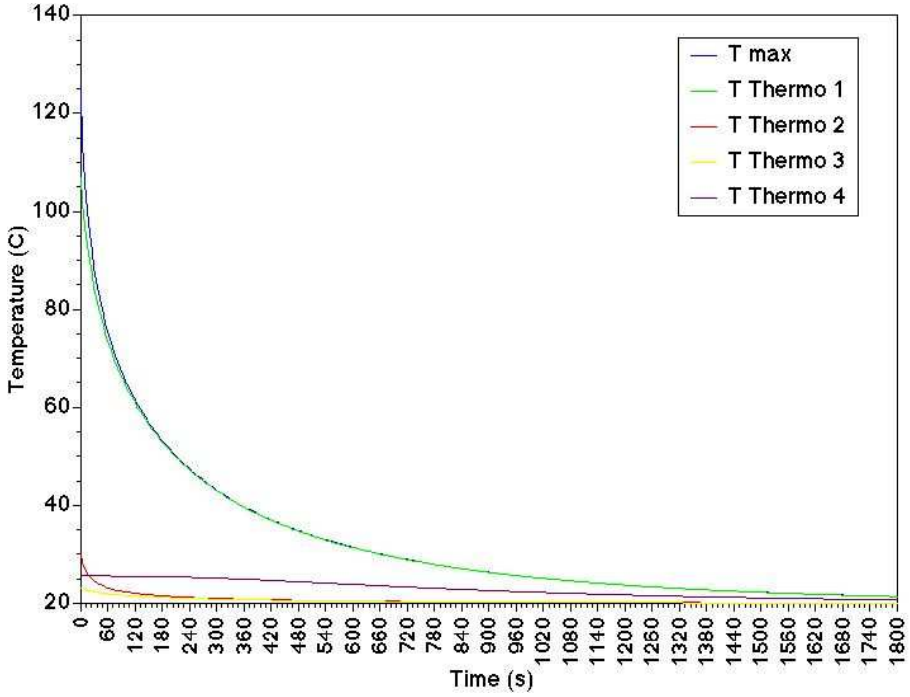

Figure 19: Case h - Temperature in relevant locations inside the target during a 30 minutes transient without the source term starting from case b steady-state solution.

6 Conclusions

A 3D thermal analysis of the target system in both steady-state and transient conditions has been performed using the finite volume commercial code StarCD coupled with the results from Fluka simulations.

Results show that the maximum temperature inside the lead target using the beam parameters of the TOF commissioning phase, and 4 pulses every super-cycle is 127 ^{o}C at steady-state operations, which is an acceptable value, compatible with safe an durable target operation. A significant improvement could be obtained with a doubled beam size (108 ^{o}C maximum temperature in the bulk of the central block).

The transients coming from the pulsed operation are not such as to create structural problems related to thermal fatigue. It is interesting to notice that the thermal oscillation in the hottest point in the bulk of the central block is much lower in the case where the 4 pulses occur at 3.6 s of distance during a PS super-cycle.

7 References

[1] S. Andriamonje et al., "Neutron TOF Facility (PS 213) - Technical Design Report", CERN/INTC/2000-004, 6 march 2000.

[2] G. Fotia, F. Maggio, L. Massidda, "Simulation of the elastic wave propagation induced by the PS beam into the TOF target at CERN", CRS4 Technical report.

[3] H. Arnould et al., “Experimental verification of neutron phenomenology in lead and transmutation by adiabatic resonance crossing in accelerator driven systems”, Physics Letters B 458 (1999) 167-180.

[4] Fassó et al., "Intermediate Energy nuclear data: models and codes". Proceedings of a specialists' meeting at Issy les Moulinex (France) 30 May - 1 June 1994, p. 271 (published by OECD, 1994).

[5] "STAR-CD Version 3.0 Manuals", Computational Dynamics, 1997.